



Performance Comparison of DSSCs-based Solid Electrolyte with Different Counter Electrodes

Erma Surya Yuliana¹, Nasikhudin¹, Nurul Hidayat¹, Arif Hidayat¹, Nandang Mufti^{1,2,*}

¹ Department of Physics, Faculty of Mathematics and Natural Sciences, Universitas Negeri Malang, Malang 65145, Indonesia

² Center of Advanced Material for Renewable Energy, Universitas Negeri Malang, Malang, 65145, Indonesia

*Corresponding Author's E-mail: nandang.mufti.fmipa@um.ac.id

Received
15 August 2024

Revised
1 October 2024

Accepted for Publication
16 October 2024

Published
31 October 2024



This work is licensed
under a [Creative
Commons Attribution-
ShareAlike 4.0
International License](https://creativecommons.org/licenses/by-sa/4.0/)

Abstract

The counter electrode (CE) in dye-sensitized solar cells (DSSCs) has an essential impact on the photovoltaic performance and long-term stability of DSSCs. Carbon materials, such as activated carbon (AC) and graphene, are attractive candidates for CE materials in DSSCs due to their low cost, high thermal conductivity, and high specific surface area. In this work, the manufacture of carbon CE using the knife coating method. Then, its performance was tested using a solar simulator and electrochemical impedance spectroscopy (EIS) testing. The samples with carbon and graphene counter electrodes show efficiencies of 0.29% and 0.23%, respectively. The findings revealed that the CE-based carbon materials had a significant impact on the performance of DSSCs. The proposed carbon materials, having low-cost fabrication, high conductivity, high thermal stability, and good corrosion resistance to electrolytes, may offer a promising solution for solar cell applications

Keywords: Activated Carbon, Graphene, Counter Electrode, Photovoltaic Performance, DSSCs.

1. Introduction

DSSCs provide the basis for energy conversion by injecting electrons from the photoexcited state of a sensitizer dye into the conduction band of a semiconductor during light absorption [1]. DSSCs consist of three main components: a dye-coated semiconductor layer on a transparent conductive glass substrate, an electrolyte, and a CE. The CE collects electrons from an external circuit and catalyzes redox electrolyte reduction and hole transport in the solid electrolyte [2]. In DSSCs, the CE is a crucial component because of its role in collecting electrons from the external load and facilitating electron exchange to catalyze the redox couple in the electrolyte. CE commonly used in DSSCs is platinum (Pt), due to its high charge transport conductivity and excellent catalytic activity for efficient regeneration of the redox couple. In addition to Pt material, carbon-based CE have attracted interest due to their ease of fabrication, good corrosion resistance, and lower cost compared to platinum electrodes [3].

The carbon material that is currently being developed is activated carbon (AC). AC has been evaluated as the most promising candidate for an alternative CE due to its relative stability, good electrical conductivity, electrochemical stability in electrolytes, low cost, and environmental friendliness [4]. Akman and Karapinar have synthesized AC-based CE and achieved a power conversion efficiency (PCE) of up to 5.67% [5]. Another study by Husain et al. with nitrogen doping on AC produced a PCE of up to 5.84% [6]. In addition to AC, carbon-based materials such as graphene can also be applied as CE. Graphene is in high demand due to its large surface area, high electrical conductivity, and excellent electrocatalytic properties. Zhang et.al. have developed graphene nanosheets. Zhang reported that graphene electrodes provide significant improvements in the photovoltaic performance of DSSC devices. The power conversion efficiency of DSSCs produced from TiO₂ nanotube photoanodes and graphene as counter electrodes is 6.81% [7].

2. Methods

The DSSC device fabrication involved two distinct preparation steps. For the first step, prepare the photoanode. Indium tin oxide (ITO) conductive glass was used. Titanium dioxide (TiO_2) mesoporous was prepared earlier by grinding TiO_2 powder with nitric acid (HNO_3), polyethylene glycol (PEG), and a few drops of Triton X-100 emulsification agent. The prepared TiO_2 paste was then spread on the ITO glass with an active area of 1 cm^2 . Then, sintering was performed at 100°C , 300°C , and 500°C for 15, 15, and 30 minutes on the hot plate. The TiO_2 working electrode was left to cool before being dipped in 0.5 mM of dye ruthenium (N-719) for 17 h. Next, a solid electrolyte based on ZnO/YSZ was coated by the doctor blade method.

For the second step, prepare the CE. CE-based carbon was prepared by mixing 0.2 grams of graphene or AC powder with 0.2 grams of polyvinylidene fluoride (PVDF), dissolved in 2 mL of N-methyl-2-pyrrolidone (NMP). The mixture was stirred at a speed of 600 rpm for 24 hours. Next, carbon paste was deposited on the silicon wafer substrate using the knife coating method and heated for 1 hour at a temperature of 100°C . Then, thin films were fabricated with a photoanode (ITO/ TiO_2 /YSZ) using the sandwich method. The samples were then tested for performance using a solar simulator and a current-voltage (I-V) photoresponse measurement. Electrochemical impedance spectroscopy (EIS) was used to determine the conductivity. An illustration of the DSSC device is shown in Figure 1.

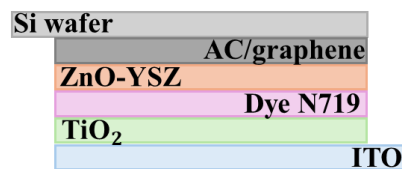


Figure 1. Illustration of the DSSCs Device Based on a Carbon Counter Electrode.

3. Results and Discussion

CE can affect the fill factor value, which describes the charge transfer resistance and catalytic activity. This affects the efficiency of solar cells. If the catalytic activity is significant, the efficiency will increase [8], [9], [10]. I-V testing of ITO/ TiO_2 /YSZ-ZnO films with CE variations using a solar simulator connected to PECCell software. Figure 2 is the result of fitting the solar cell I-V measurement.

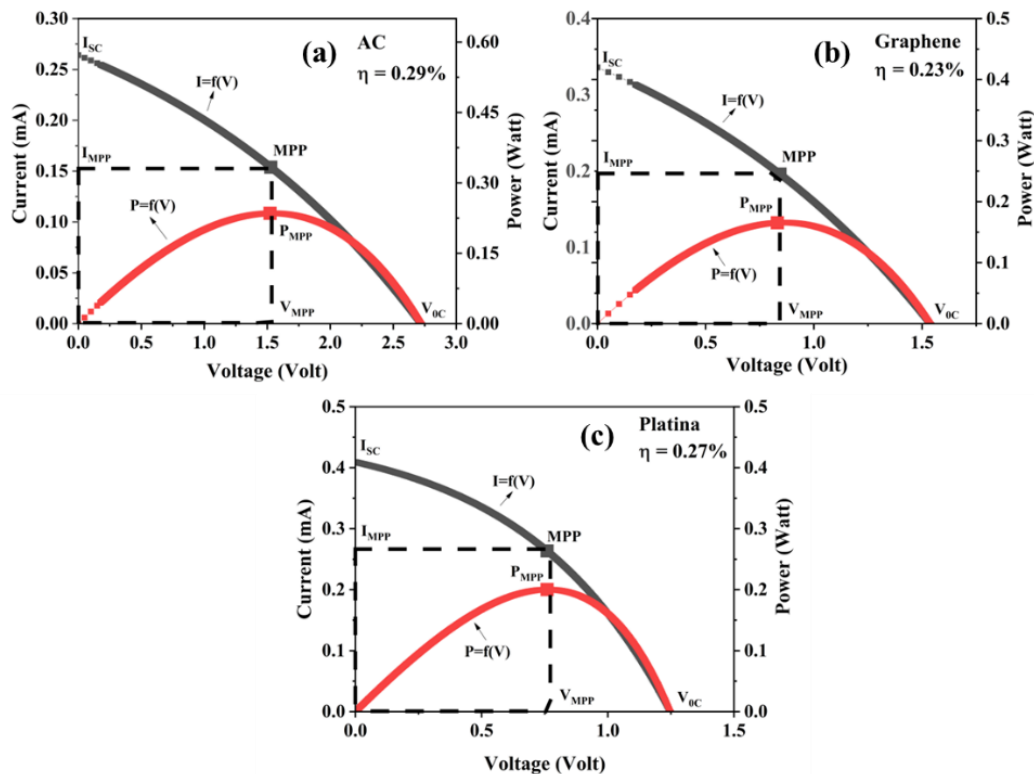


Figure 2. Efficiencies of DSSCs with Variations in the Counter Electrode (a) AC, (b) Graphene, and (c) Platinum.

The efficiency parameters of DSSCs with variations in temperature and counter electrode are summarized in Table 1. Based on Table 1, the J_{sc} , V_{oc} , V_{max} , and P_{max} values of DSSCs with an AC counter electrode are greater than the J_{sc} , V_{oc} , V_{max} , and P_{max} values with graphene and Pt as counter electrodes. When the variables are significant, high efficiency is obtained and becomes a benchmark for solar cell performance. The fill factor influences the size of the efficiency value. The low FF is caused by the considerable charge transfer resistance that occurs at the counter electrode [10]. The FF value is influenced by the series resistance (R_s) and shunt resistance (R_{sh}), where these two resistances act in opposite directions. A low FF value is caused by an increasing R_s value in the DSSC and a decreasing R_{sh} value. As the R_s value in the DSSC increases, the J_{sc} value decreases, resulting in a decrease in the energy conversion efficiency of these DSSCs. Furthermore, the FF value in these DSSCs is also influenced by the catalytic activity of the counter electrode [11]. The efficiency of the $TiO_2/YSZ-ZnO$ DSSCs cell with an AC counter electrode was 0.29%, while the graphene and Pt counter electrodes were 0.23% and 0.10%, respectively. This efficiency is similar to the study by Ansar *et al.*, where the use of a carbon counter electrode in solar cells resulted in an efficiency of <0.5% [12].

In addition to efficiency, the size of the performance can also be determined by analyzing the sample's response to light, also known as its photoresponse. DSSCs films with various counter electrodes, having an area of $1 \times 2 \text{ cm}^2$, were measured for photoresponse using a solar simulator as a light source with a power input of 100 mW/cm^2 for several minutes with an on and off interval of every 5 seconds. Figure 3 shows the graph of voltage and current photoresponse as a function of time for DSSCs with different counter electrodes. Voltage and current measurements were taken in both dark and bright conditions, with measurements taken every 5 seconds.

Table 1. DSSCs Efficiency Parameters on Counter Electrode Variations.

Sample	Platina	Graphene	AC
I_{sc} (mA)	0.07	0.07	0.07
J_{sc} (mA/cm ²)	0.27	0.28	0.29
V_{oc} (V)	1.48	1.44	2.55
Fill factor	0.67	0.56	0.39
P_{max} (W)	0.07	0.06	0.07
I_{max} (mA)	0.06	0.06	0.04
V_{max} (V)	1.05	0.95	1.95
η (%)	0.27	0.23	0.29

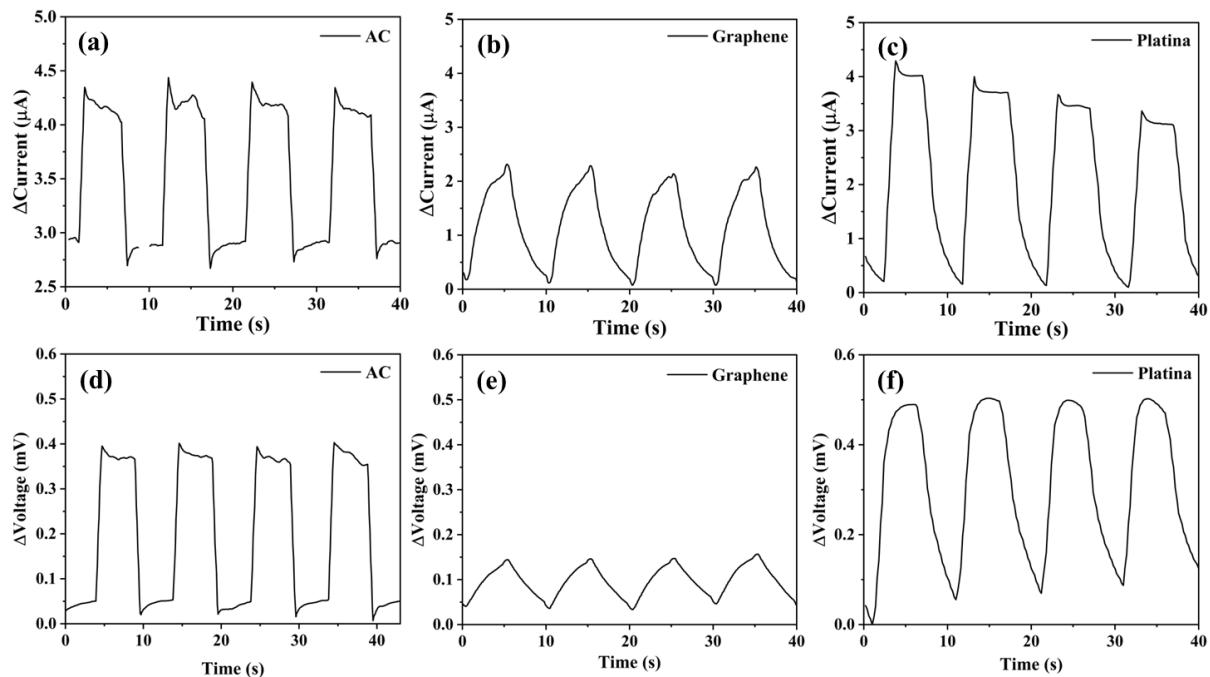


Figure 3. Photoresponse Graphs of (a-c) Current-Time and (d-e) Voltage-Time Function for DSSCs with Various Counter Electrodes.

Figure 4 shows that DSSCs with varying CEs have a good response to light. When the film is exposed to light from a solar simulator, there is a rapid increase in photoresponse current and voltage. When not exposed to light, the film responds well without reaching saturation [13]. The graphs illustrate the differences in photoresponse current and voltage. This is likely due to the differences in the CE materials used [14].

The results of the I-t fitting of the photoresponse of the ITO/TiO₂/YSZ-ZnO film with variations of counter electrodes, Pt, AC, and graphene, are shown in Figure 4 and Table 2. Based on the analysis obtained, the time required for the film to respond to light when light is on is faster than when light is off. This is due to the formation of a trap state by light, which hampers the movement of photogenerated carriers when the light is off. The DSSCs sample with AC as CE exhibits the fastest response time when exposed to light, specifically 0.37 s when light is on and 0.73 s when light is off. Previous research stated that a good solar cell has a speed in responding to light of no more than 2 s [15], [16]. So, AC as a counter electrode can produce better performance of solid electrolyte-based DSSCs compared to CE Pt and graphene.

Table 2. Photoresponse Result Parameters of DSSCs with CE Variations

Sample	Δ Current (μ A)	Δ Voltage (mV)	Light on (τ_{up}) (s)	Light off (τ_{down}) (s)
Platina	4.26	0.49	0.66	1.56
AC	4.41	0.40	0.37	0.73
Graphene	2.31	0.16	2.94	3.80

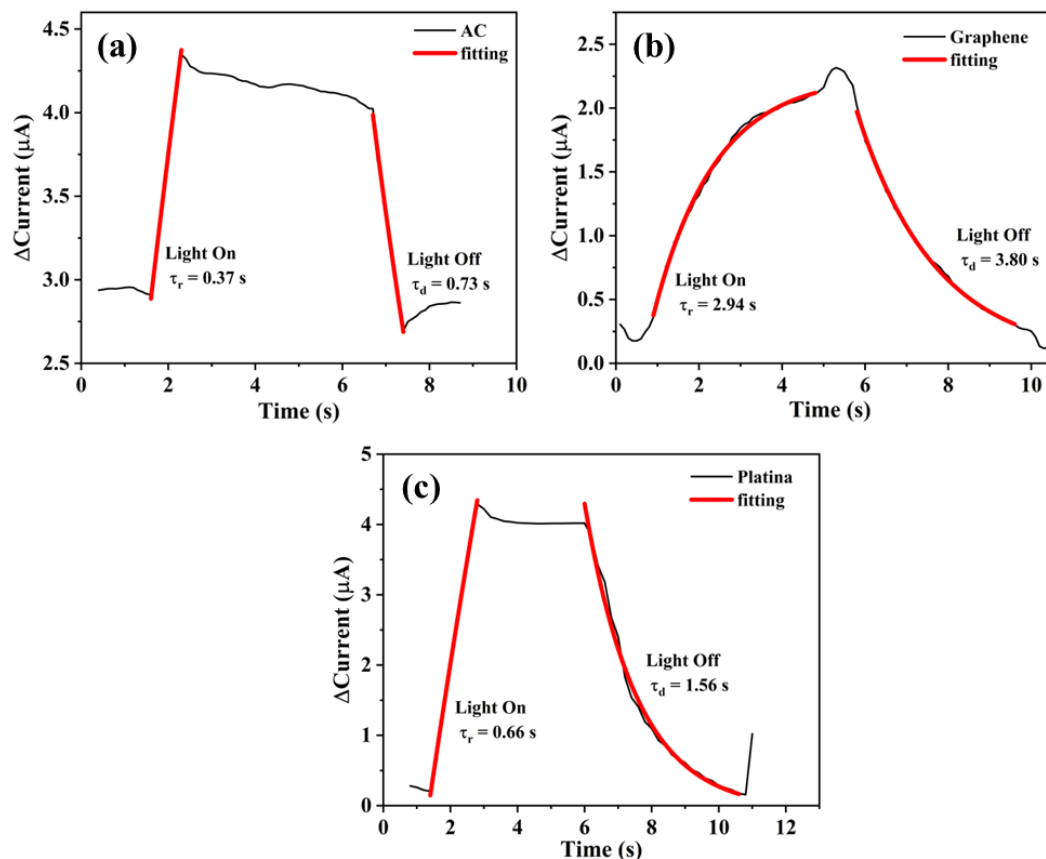


Figure 4. Fitting the Current Photoresponse of DSSCs with Variations in Counter Electrode (a) AC, (b) Graphene, and (c) Platina.

EIS was used to show the differences in charge transfer from DSSCs with temperature variations of 650°C on three different counter electrodes. Nyquist plots resulting from ion transport with low electrolyte resistance have been observed. Charge transfer resistance occurs in a semicircular shape, characterized by a high frequency at the electrolyte interface and carbon counter electrode. Electron transfer resistance, on the other hand, occurs at the interface between the electrolyte, dye, and TiO₂

electrode. The solid electrolyte used consists of zinc oxide semiconductor material and YSZ ceramic material. Both materials exhibit good conductivity, so the composite of the two is expected to enhance the conductivity of the solid electrolyte used. Conductivity calculations can be performed using the following equation 1:

$$\sigma_t = \frac{L}{(R_0 + R_1) \times A} \tag{1}$$

where L is the electrolyte thickness (22.7 μm), and A is the effective area of the DSSCs of 0.25 cm².

The EIS curve of DSSCs with CE-based carbon is shown in Figure 5. The equivalent circuit is used for fitting the EIS data, where R₁, R₂, and R₄, constant phase element (CPE) represents ohmic resistance, ionic grain boundary resistance, charge transfer resistance, and CPE, respectively. R_s (R₁) is the series resistance/transport resistance and depends on the conductivity of the material. Solid electrolytes have a recombination resistance R_r (R₂) ten times higher in magnitude (up to kΩ), which means that ceramics can significantly avoid recombination that occurs at the TiO₂/sensitizer-electrolyte interface. This can prevent corrosion of the sensitizer due to unwanted recombination. Based on the research of solid electrolyte-based DSSCs conducted by Kusuma and Balakrishna, a lower R_{ct} (R₄) indicates that good charge transfer across the electrode interface can be observed from its high FF [17]. This study reveals lower R_r and higher R_{ct}, resulting in slightly lower performance, as indicated by efficiency data. In another study, namely a DSSCs based on a carbon counter electrode by Bayram *et al.*, R_{ct1} (R₂) represents the charge-transfer resistance at the counter electrode/electrolyte interface, and R_{ct2} (R₄) represents the charge-transfer resistance at the TiO₂/dye/electrolyte interface. The CPE results obtained are around 0.03% [18].

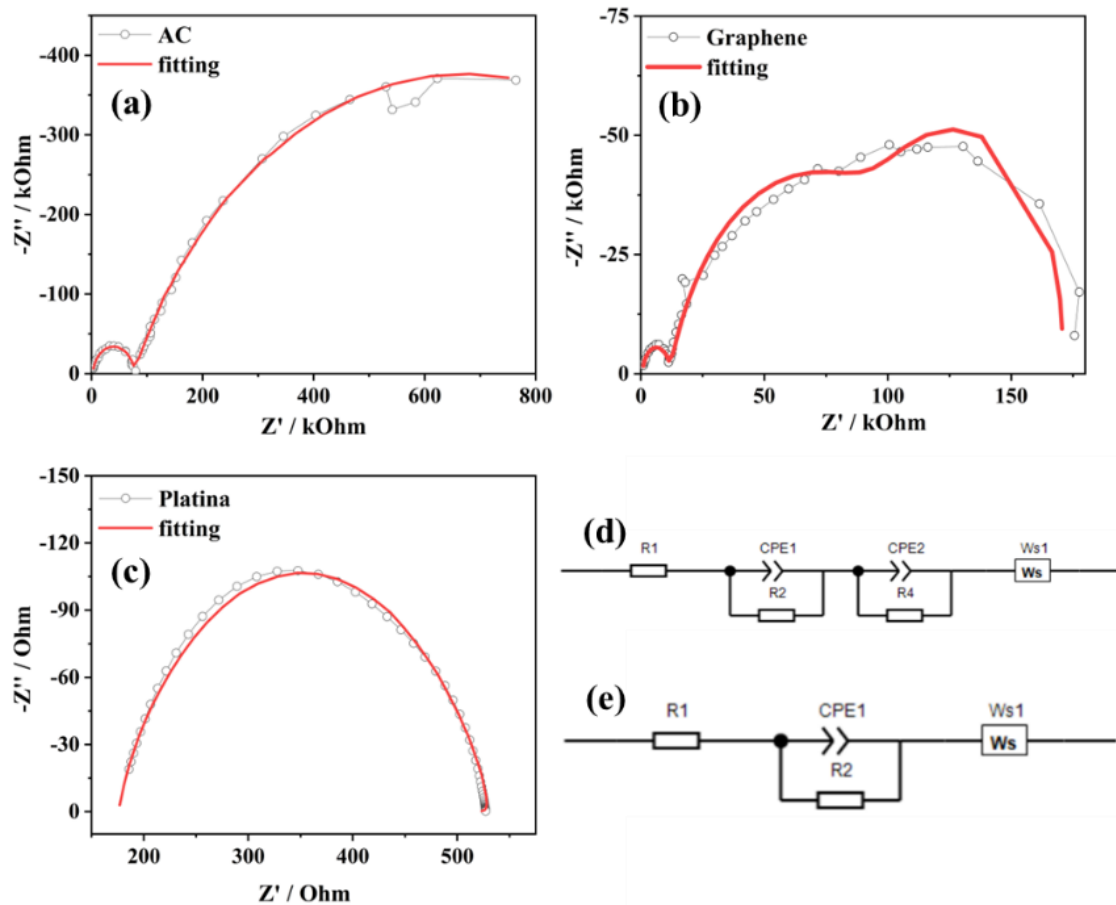


Figure 5. Nyquist Curve Plots of DSSCs with (a) AC, (b) Graphene, and (c) Pt Counter Electrode, (d) Circuit Model for AC and Graphene Impedance, (d) Pt Impedance Fitting Circuit Model.

Based on these data, the results of the calculation of the total ionic conductivity (σ_t) of the relevant DSSCs are also listed in Table 3. The electrical conductivity value affects the performance of the

counter electrode. If the counter electrode is good, the resulting electrical conductivity will be high [19]. Based on the calculation, the conductivity of the DSSCs with a platinum counter electrode produces a maximum value of $10.195 \mu\text{S cm}^{-1}$. This finding is in line with the CPE obtained, which is still low at $<0.3\%$.

Tabel 3. EIS Fitting Results of DSSCs with Counter Electrode Variations.

Sample	R_0 (ohm cm^2)	R_1 (ohm cm^2)	R_2 (ohm cm^2)	$R_t (R_0 + R_1)$ (ohm cm^2)	σ_t ($\mu\text{S cm}^{-1}$)
Platina	606.8	283.83	-	890.63	10.195
AC	2219.8	73871	118850	76090.8	0.119
Graphene	707.82	10490	78524	11197.82	0.811

1. Conclusion

DSSC based carbon counter electrode with various carbon materials was prepared and characterized. Based on the DSSC characterization analysis, AC had a good physical appearance compared with the other samples in efficiency and photoresponse compare to AC conductivity although it was still low compare to Pt counter electrode. The AC was then successfully fabricated as a counter electrode for DSSCs with the combination of ITO-TiO₂ (N719 dye)/ZnO-YSZ. Briefly, the present work may constitute a basis for future high performance DSSCs based carbon counter electrode.

Acknowledgment

This research was supported by DRTPM Kemendikbudristek 2024 under Grant No. 11.6.103/UN32.14.1/LT/2024. The authors gratefully acknowledge the financial support that made this work possible.

References

- [1] E. Surya Yuliana, A. Chairani Alvin Nadhira, N. Mufti, M. Diantoro, and P. Puspitasari, "A Brief Study of the Carbon Counter Electrode for Photosensor based on DSSC," E3S Web Conf., vol. 473, pp. 0–6, 2024, doi: 10.1051/e3sconf/202447301005.
- [2] S. Ding, C. Yang, J. Yuan, H. Li, X. Yuan, and M. Li, "An overview of the preparation and application of counter electrodes for DSSCs," RSC Adv., vol. 13, no. 18, pp. 12309–12319, 2023, doi: 10.1039/D3RA00926B.
- [3] N. Narudin, P. Ekanayake, Y. W. Soon, H. Nakajima, and C. M. Lim, "Enhanced properties of low-cost carbon black-graphite counter electrode in DSSC by incorporating binders," Sol. Energy, vol. 225, pp. 237–244, Sep. 2021, doi: 10.1016/j.solener.2021.06.070.
- [4] K. D. M. S. P. K. Kumarasinghe, G. R. A. Kumara, R. M. G. Rajapakse, D. N. Liyanage, and K. Tennakone, "Activated coconut shell charcoal based counter electrode for dye-sensitized solar cells," Org. Electron., vol. 71, pp. 93–97, Aug. 2019, doi: 10.1016/j.orgel.2019.05.009.
- [5] E. Akman and H. S. Karapinar, "Electrochemically stable, cost-effective and facile produced selenium@activated carbon composite counter electrodes for dye-sensitized solar cells," Sol. Energy, vol. 234, pp. 368–376, Mar. 2022, doi: 10.1016/j.solener.2022.02.011.
- [6] A. Husain et al., "Attaining promising efficiency through a Quasi-Solid-State symmetrical supercapacitor and Dye-Sensitized solar cell counter electrode utilizing bifunctional Nitrogen-Doped microporous activated carbon," Inorg. Chem. Commun., p. 112859, Jul. 2024, doi: 10.1016/j.inoche.2024.112859.
- [7] D. W. Zhang et al., "Graphene-based counter electrode for dye-sensitized solar cells," Carbon N. Y., vol. 49, no. 15, pp. 5382–5388, Dec. 2011, doi: 10.1016/j.carbon.2011.08.005.
- [8] X. Zhang et al., "High fill factor organic solar cells with increased dielectric constant and molecular packing density," Joule, vol. 6, no. 2, pp. 444–457, Feb. 2022, doi: 10.1016/j.joule.2022.01.006.
- [9] S. S. Patil, S. N. Nadaf, R. M. Mane, L. P. Deshmukh, and P. N. Bhosale, "One pot hydrothermal synthesis and characterization of Cu₂ZnSn(S,Se)₄ nanocrystalline thin films: Photovoltaic performance," 2021, p. 080006. doi: 10.1063/5.0043699.

- [10] M. B. A. Bashir, A. H. Rajpar, E. Y. Salih, and E. M. Ahmed, "Preparation and Photovoltaic Evaluation of CuO@Zn(Al)O-Mixed Metal Oxides for Dye Sensitized Solar Cell," *Nanomaterials*, vol. 13, no. 5, p. 802, Feb. 2023, doi: 10.3390/nano13050802.
- [11] A. C. A. Nadhira *et al.*, "The brief study of ZnO/PEDOT:PSS counter electrode in DSSC Based on solid electrolyte YSZ," *Mater. Sci. Energy Technol.*, vol. 7, no. April, pp. 309–317, 2024, doi: 10.1016/j.mset.2024.04.003.
- [12] F. Ansar, N. Mufti, and M. T. H. Abadi, "The Effect of Counter on Thin Film ZnO Nanorods on the Performance of Solar Cell based on Photoelectrochemical cell," no. November 2016, 2023.
- [13] K. Keem *et al.*, "Photocurrent in ZnO nanowires grown from Au electrodes," *Appl. Phys. Lett.*, vol. 84, no. 22, pp. 4376–4378, May 2004, doi: 10.1063/1.1756205.
- [14] Y. Wang *et al.*, "Investigation of the Photoresponse and Time-Response Characteristics of HDA-BiI₅-Based Photodetectors," *Materials (Basel)*, vol. 15, no. 1, p. 321, Jan. 2022, doi: 10.3390/ma15010321.
- [15] Z. Zhang *et al.*, "Lateral Photocurrent-Induced High-Performance Self-Powered Photodetector Observed in CIGS Heterojunction," *IEEE Trans. Electron Devices*, vol. 67, no. 4, pp. 1639–1644, 2020, doi: 10.1109/TED.2020.2976665.
- [16] J. Gong *et al.*, "Enhancing photocurrent of Cu(In,Ga)Se₂ solar cells with actively controlled Ga grading in the absorber layer," *Nano Energy*, vol. 62, pp. 205–211, Aug. 2019, doi: 10.1016/j.nanoen.2019.05.052.
- [17] J. Kusuma and R. Geetha Balakrishna, "Ceramic grains: Highly promising hole transport material for solid state QDSSC," *Sol. Energy Mater. Sol. Cells*, vol. 209, p. 110445, Jun. 2020, doi: 10.1016/j.solmat.2020.110445.
- [18] O. Bayram *et al.*, "Graphene/polyaniline nanocomposite as platinum-free counter electrode material for dye-sensitized solar cell: its fabrication and photovoltaic performance," *J. Mater. Sci. Mater. Electron.*, vol. 31, no. 13, pp. 10288–10297, Jul. 2020, doi: 10.1007/s10854-020-03575-5.
- [19] G. Li and X. Gao, "Low-Cost Counter-Electrode Materials for Dye-Sensitized and Perovskite Solar Cells," *Adv. Mater.*, vol. 32, no. 3, Jan. 2020, doi: 10.1002/adma.201806478.